Tetrahedron 67 (2011) 9112–9121

Contents lists available at SciVerse ScienceDirect

Tetrahedron

journal homepage: www.elsevier.com/locate/tet

Absolute stereochemistry of antifouling cembranoid epimers at C-8 from the Caribbean octocoral *Pseudoplexaura flagellosa*. Revised structures of plexaurolones

Edisson Tello [a], Leonardo Castellanos [a], Catalina Arevalo-Ferro [b], Jaime Rodríguez [c], Carlos Jiménez [c], Carmenza Duque [a,*]

[a] Departamento de Química, Universidad Nacional de Colombia, AA 14490 Bogotá, Colombia
[b] Departamento de Biología, Universidad Nacional de Colombia, AA 14490 Bogotá, Colombia
[c] Departamento de Química Fundamental, Universidade da Coruña, E-15071 A Coruña, Spain

ARTICLE INFO

Article history:
Received 20 July 2011
Received in revised form 14 September 2011
Accepted 20 September 2011
Available online 25 September 2011

Keywords:
Pseudoplexaura flagellosa
Cembranes
Plexaurolones
Antifouling
Bacterial biofilm inhibition
Quorum sensing inhibition

ABSTRACT

Eight cembranoid epimers at C-8 (**1**–**8**) were isolated from the organic extract of the Colombian Caribbean octocoral *Pseudoplexaura flagellosa*. Compounds **2**, **4**, and **6** are reported for the first time. Although compounds **1**, **3**, **5**, **7**, and **8** have been reported previously, their structures and NMR assignments are revised, completed or corrected. The structures of these compounds were established on the basis of detailed analysis of their spectroscopic data. Furthermore, the relative configurations of compounds **1**–**3** and **7** were confirmed by single-crystal X-ray diffraction. The absolute configurations of compounds **1**–**8** were determined using a combination of the modified Mosher method and unambiguous chemical interconversions. Evaluation of their antifouling properties using quorum sensing inhibition (QSI) and biofilm inhibition bioassays showed that compounds **3**, **6**, and **7** have excellent QSI activity against *Chromobacterium violaceum*, as measured by inhibition of the production of violacein pigment, without interfering with its growth. Furthermore, compounds **3**, **5**, **6**, and **8** exhibited inhibition of biofilm maturation without interfering in the growth of *Pseudomonas aeruginosa*, *Vibrio harveyi*, and *Staphylococcus aureus*. This is the first report of cembranoids as inhibitors of bacterial biofilm and as compounds that interfere with QS in *C. violaceum*.

1. Introduction

Recent developments in the study of antifouling agents have focused on marine natural products that provide nontoxic compounds that could be incorporated into environmentally friendly antifouling paints,[1] particularly since the International Maritime Organization (IMO) banned the application of organotin compounds and other potent toxic biocides (the treaty came into effect in September, 2008). Although the latter are very potent in the antifouling treatment of submerged surfaces, they are also very toxic to the marine environment. In general, the idea of these studies is to imitate the behavior of marine organisms, particularly those whose surfaces are free of fouling, by means of chemical molecules that are used to communicate and act as a defense mechanism—particularly to prevent colonization.

The antifouling properties can be evaluated using quorum sensing inhibition (QSI) and biofilm inhibition bioassays. Bacterial QS is implicated in the regulation of pathologically relevant events, such as biofilm maturation, bacterial virulence, and drug resistance.[2] Inhibitors of bacterial quorum sensing could therefore be useful therapeutics and fouling controllers.

Furthermore, with this idea in mind, and as a part of our continued search for antifouling compounds from marine organisms of the Colombian Caribbean Sea,[3–5] we examined the gorgonian octocoral *Pseudoplexaura flagellosa*, which is very abundant in the Santa Marta Bay region. Our preliminary assays using marine bacteria (microfouling) associated with heavily fouled marine sources indicated the presence of antifouling compounds in the non-polar extract of this animal.

P. flagellosa collected near Pigeon Key (Florida) has been chemically examined by several authors[6,7] and a complex mixture of sesquiterpene hydrocarbons, crassin acetate, and an inseparable mixture of two 4α-methylsterols was found. However, this is the first time that specimens collected in the Colombian Caribbean Sea have been studied in an effort to ascertain their chemical composition and their antifouling properties. On the other hand, some of the diterpenes reported in this work have structures related to plexaurolone, dihydroplexaurolone, and dehydroplexaurolone, which were previously isolated from *Plexaura* sp.[8,9] However, in some cases the relative and/or absolute configurations of these compounds remained unknown and in other cases they needed to

* Corresponding author. Tel.: +571 3165000x14477; fax: +571 3165220; e-mail address: cduqueb@unal.edu.co (C. Duque).

0040-4020/$ – see front matter © 2011 Elsevier Ltd. All rights reserved.
doi:10.1016/j.tet.2011.09.094

be reexamined. Information about chemical structure elucidation in the literature, particularly the configuration of C-8 for plexaurolone, is confusing—as exemplified by the 8*S* configuration reported by Ealick et al.[8] and the wrongly depicted 8*R* configuration reported by Chan et al.[9]

In this paper we describe the isolation from *P. flagellosa* of four pairs of cembrane epimers at C-8 and report the elucidation of their structures, including the absolute configuration of their chiral centers. In addition, we also report quorum sensing inhibition (QSI) and biofilm inhibition activities for the aforementioned compounds. The aim of these investigations was to establish whether these compounds have the ability to interfere with the bacterial signal-mediated quorum sensing systems involved in biofilm maturation and microbial surface colonization, which are the first steps of the fouling process.

2. Results and discussion

Frozen material of *P. flagellosa*, collected at Santa Marta Bay, Colombian Caribbean, was extracted with CH_2Cl_2/MeOH (1:1 v/v) and the crude extract obtained after evaporation of the solvent was partitioned between CH_2Cl_2/H_2O (1:1 v/v). The resulting active organic fraction (on QSI bioassay) was subjected to chromatography on silica gel and final purification by RP-HPLC to afford pure compounds **1**–**8**. In the case of compounds **1**–**3** and **7**, crystallization was also used as a final purification step.

Compound **1** was isolated as white crystals and has a molecular formula $C_{20}H_{34}O_3$, assigned on the basis on its HRESIMS pseudomolecular ion at *m/z* 345.2385 $[M+Na]^+$ (Δ 6.1 ppm). The ^1H NMR, ^{13}C NMR, and IR data of **1** were indicative of a cembrane-type structure[10,11] and are consistent with those reported for plexaurolone previously isolated from another octocoral referred to as *Plexaura A*.[8,9] However, the bibliographic data available did not show the unequivocal assignment of NMR signals or clearly show the absolute stereochemistry, as evidenced by two contradictory reports, 8*S* reported by Ealick et al.[8] and 8*R* reported by Chan et al.[9] Analysis of the 2D NMR ($^1H-^1H$ COSY, gHMQC, and gHMBC) spectra of **1** allowed us to relate all the protons to their corresponding carbons and assign all of the NMR signals (Tables 1 and 2, Fig. 1). A detailed study of the spatial configuration of **1** using NOESY experiments, the modified Mosher method and the X-ray diffractogram for this compound was pursued. Some key NOE correlations led us to establish the relative configuration of **1** as 1*R**,3*R**,4*R**,8*S**,12*R**, particularly the cross-peaks between H-3 and H-1 and H-3 and H-1/H_3-18, and analysis of the ORTEP diagram obtained by single-crystal X-ray diffraction (Fig. 2). The absolute configuration at C-3 of compound **1** was established as *R* by using the modified Mosher methodology with methoxyphenylacetic acid (MPA) as a derivatization reagent for the hydroxyl group present in C-3.[12,13] Selected chemical shift differences ($\Delta\delta^{RS}$) for the (*R*)- and (*S*)-MPA esters of **1** at C-3 (**1a** and **1b**, respectively) are summarized in Table 3. Thus, the overall analysis led us to establish the structure of **1** as (1*R*,3*R*,4*R*,8*S*,12*R*)-6,11-diketocembra-15(17)-en-3-ol [(8*S*)-plexaurolone]. The stereostructure of compound **1** is identical to that published by Ealick et al.[8] but it was wrongly depicted by Chan et al.[9]

Compound **2** was obtained as white crystals with a molecular formula of $C_{20}H_{34}O_3$ assigned on the basis of the HRESIMS pseudomolecular ion at *m/z* 345.2386 $[M+Na]^+$ (Δ 5.8 ppm) and ^{13}C NMR spectra, which showed 4° of unsaturation. The IR spectrum revealed the presence of hydroxyl, two carbonyl and olefinic bands at 3417, 1697, 1643, and 879 cm^{-1}, respectively. The NMR spectroscopic features of **2** were similar to those of **1** (Tables 1 and 2), i.e., the data also revealed 20 carbon signals for a cembrane-type diterpene, including the presence of three methyl groups (δ_H 1.02, d, *J*=6.9 Hz/δ_C 15.5; δ_H 0.98, d, *J*=7.0 Hz/δ_C 21.2; δ_H 0.94, d, *J*=6.6 Hz/δ_C 14.2), an isopropenyl group (δ_H 4.74, br s, 4.70, br s, δ_C 110.2, CH_2; δ_H 1.69, s, δ_C 20.8, CH_3; δ_C 149.0, qC), one hydroxy-bearing methine (δ_H 3.34, d, *J*=10.4 Hz, δ_C 72.0, CH) and two ketone groups (δ_C 214.5, qC and δ_C 211.6, qC). Analysis of $^1H-^1H$ COSY and gHMBC data allowed us to assign the NMR signals for **2** (Tables 1 and 2, Fig. 1) and to establish that compound **2** has the same planar structure as **1**. However, slight differences in the NMR data of these two compounds, particularly in the signals assigned to CH_2-5 (δ_H 2.37, m, 2.23, m, δ_C 48.2, in **1**; δ_H 2.74, m, 2.65, m, δ_C 47.7, in **2**), CH_2-7 (δ_H 2.53, m, 2.30, m, δ_C 48.3, in **1**; δ_H 2.64, m, 2.52, m, δ_C 47.7, in **2**) and CH_2-9 (δ_H 1.48, m, 1.24, m, δ_C 29.2, in **1**; δ_H 1.53, m, 1.36, m, δ_C 28.4, in **2**) indicated that **2** is a stereoisomer of **1**. In addition, key NOE correlations, particularly the cross-peaks between H-12 and H-8, H-3 and H-1/H_3-18, and the results of single-crystal X-ray diffraction analysis (Fig. 2) clearly establish the relative stereochemistry of **2** as 1*R**,3*R**,4*R**,8*R**,12*R**. Finally, the absolute configuration at C-3 of compound **2** was established as *R* by using the modified Mosher methodology with MPA as the

Table 1
^{13}C NMR Spectroscopic data (100 MHz, $CDCl_3$) for compounds **1**–**9**

Compounds	**1**	**2**	**3**[a]	**4**	**5**	**6**	**7**	**8**	**9**
Position	δ_C, mult.[b]	δ_C, mult.[b]	δ_C, mult.[b]	δ_C, mult.[b]	δ_C, mult.[b]	δ_C, mult.[b]	δ_C, mult.[b]	δ_C, mult.[b]	δ_C, mult.[b]
1	43.0, CH	42.8, CH	41.8, CH	41.7, CH	46.8, CH	46.2, CH	41.4, CH	41.1, CH	43.5, CH
2	39.0, CH_2	38.0, CH_2	38.1, CH_2	37.9, CH_2	29.4, CH_2	29.1, CH_2	30.0, CH_2	30.8, CH_2	25.4, CH_2
3	70.7, CH	72.0, CH	70.1, CH	70.1, CH	33.8, CH_2	34.3, CH_2	215.6, qC	215.1, qC	79.0, CH
4	37.1, CH	36.7, CH	36.5, CH	36.5, CH	28.1, CH	27.0, CH	47.2, CH	47.3, CH	37.4, CH
5	48.2, CH_2	47.7, CH_2	48.8, CH_2	49.0, CH_2	37.4, CH_2	35.9, CH_2	31.6, CH_2	31.1, CH_2	46.5, CH_2
6	211.4, qC	211.6, qC	211.3, qC	211.8, qC	210.6, qC	210.6, qC	210.4, qC	210.7, qC	109.7, qC
7	48.3, CH_2	47.7, CH_2	47.9, CH_2	47.9, CH_2	50.9, CH_2	50.8, CH_2	49.5, CH_2	50.9, CH_2	50.7, CH_2
8	27.4, CH	27.3, CH	38.4, CH	38.2, CH	31.4, CH	30.2, CH	29.5, CH	27.1, CH	36.3, CH
9	29.2, CH_2	28.4, CH_2	30.6, CH_2	30.5, CH_2	31.6, CH_2	31.0, CH_2	32.1, CH_2	32.1, CH_2	39.2, CH_2
10	36.3, CH_2	36.4, CH_2	29.4, CH_2	29.2, CH_2	47.8, CH_2	50.5, CH_2	36.7, CH_2	38.3, CH_2	33.1, CH_2
11	214.4, qC	214.5, qC	75.0, CH	75.1, CH	214.7, qC	214.7, qC	214.4, qC	214.4, qC	70.4, CH
12	46.9, CH	46.9, CH	28.1, CH	28.2, CH	46.9, CH	47.3, CH	41.5, CH	42.6, CH	29.1, CH
13	31.2, CH_2	30.6, CH_2	29.0, CH_2	29.0, CH_2	29.5, CH_2	29.6, CH_2	47.4, CH_2	46.7, CH_2	30.4, CH_2
14	29.5, CH_2	29.8, CH_2	27.2, CH_2	27.1, CH_2	30.2, CH_2	29.7, CH_2	46.4, CH_2	46.7, CH_2	24.1, CH_2
15	148.7, qC	149.0, qC	150.2, qC	149.9, qC	147.8, qC	148.3, qC	147.6, qC	147.5, qC	148.5, qC
16	20.5, CH_3	20.8, CH_3	21.1, CH_3	21.3, CH_3	20.4, CH_3	20.6, CH_3	20.1, CH_3	20.3, CH_3	23.3, CH_3
17	109.9, CH_2	110.2, CH_2	109.0, CH_2	109.3, CH_2	110.0, CH_2	110.0, CH_2	110.6, CH_2	110.6, CH_2	110.4, CH_2
18	13.2, CH_3	14.2, CH_3	13.4, CH_3	13.6, CH_3	21.0, CH_3	21.1, CH_3	16.4, CH_3	16.5, CH_3	13.6, CH_3
19	21.0, CH_3	21.2, CH_3	20.9, CH_3	21.1, CH_3	20,3, CH_3	21,0, CH_3	21.5, CH_3	22.0, CH_3	24.5, CH_3
20	15.9, CH_3	15.5, CH_3	16.1, CH_3	16.2, CH_3	16.6, CH_3	15.9, CH_3	17.3, CH_3	17.2, CH_3	16.0, CH_3

[a] NMR data (125 MHz) in CD_2Cl_2.
[b] Full assignments were carried out by $^1H-^1H$ COSY, gHMQC, and gHMBC experiments.

Table 2
^{1}H NMR spectroscopic data (400 MHz, $CDCl_3$) for compounds **1**–**9**

Compounds	**1**	**2**	**3**[a]	**4**	**5**	**6**	**7**	**8**	**9**
Position[b]	δ_H, (J in Hz)	δ_H, (J in Hz)	δ_H, (J in Hz)	δ_H, (J in Hz)	δ_H, (J in Hz)	δ_H, (J in Hz)	δ_H, (J in Hz)	δ_H, (J in Hz)	δ_H, (J in Hz)
1	2.16, m	2.14, m	2.23, m	2.21, m	1.81, m	1.79, m	2.54, m	2.55, m	2.08, m
2a	1.60, m	1.53, m	1.61, m	1.61, m	1.25, m	1.34, m	1.24, m	1.03, m	2.12, m
2b	1.34, m	1.34, m	1.40, m	1.38, m			0.96, m	0.96, m	1.22, m
3a	3.33, d (9.0)	3.34, d (10.4)	3.45, ddd (9.0, 6.4, 2.7)	3.43, d (10.9)	1.08, m	1.13, m	—	—	3.95, ddd (12.6, 7.0, 2.4)
3b						1.01, m			
4	2.00, m	2.17, m	2.09, m	2.08, m	2.06, m	2.25, m	2.43, m	2.36, m	2.27, qt (14.0, 7.1)
5a	2.37, m	2.74, m	2.47, dd (15.0, 11.3)	2.44, dd (16.4, 9.8)	2.53, m	2.49, m	2.17, m	1.64, m	2.04, m
5b	2.23, m	2.65, m	2.36, m	2.31, m	2.32, m	2.18, m	1.52, m	1.57, m	1.70, m
6	—	—	—	—	—	—	—	—	—
7a	2.53, m	2.64, m	2.58, dd (16.4, 9.8)	2.59, dd (15.0, 11.3)	2.25, m	2.23, m	2.08, m	2.53, m	1.80, m
7b	2.30, m	2.52, m	2.31, m	2.26, m	2.11, m	2.11, m	2.01, m	2.27, m	1.65, m
8	2.12, m	2.20, m	1.50, m	1.49, m	1.90, m	1.48, m	1.90, m	2.12, m	1.58, m
9a	1.48, m	1.53, m	1.58, m	2.15, m	1.92, m	1.48, m	1.33, m	1.55, m	1.74, m
9b	1.24, m	1.36, m	1.27, m				0.89, m	1.36, m	1.13, m
10a	2.49, m	2.42, m	1.48, m	1.42, m	2.13, m	2.35, m	2.94, m	2.41, m	1.57, m
10b	2.23, m	2.33, m	1.40, m	1.17, m	2.06, m	2.30, m	2.47, m	2.32, m	1.44, m
11	—	—	3.32, d (10.9)	3.31, ddd (9.0, 6.4, 2.7)	—	—	—	—	4.01, dd (10.5, 4.2)
12	2.47, m	2.47, m	2.10, m	2.08, m	2.47, m	2.42, m	3.20, dd, (7.2, 3.0)	3.20, ddt, (11.0, 7.0, 3.5)	1.60, m
13a	1.46, m	2.22, m	1.48, m	1.40, m	1.10, m	1.11, m	2.52, m	2.98, dd, (16.4, 11.3)	1.51, m
13b	1.44, m	1.46, m	1.17, m	1.16, m			2.43, m	2.15, m	1.29, m
14a	1.69, m	2.16, m	1.44, m	1.52, m	1.10, m	1.22, m	3.20, m	2.80, m	2.47, td (10.1, 5.3)
14b	1.16, m	1.35, m	1.31, m	1.47, m			2.20, m	2.71, m	1.31, m
15	—	—	—	—	—	—	—	—	—
16	1.66, s	1.69, s	1.75, s	1.70, s	1.63, s	1.61, s	1.68, s	1.66, s	1.75, s
17a	4.71, br s	4.74, br s	4.75, br s	4.70, br s	4.70, s	4.68, s	4.72, br s	4.71, br s	4.88, br s
17b	4.66, br s	4.70, br s	4.69, br s	4.64, br s	4.62, s	4.59, s	4.72, br s	4.70, br s	4.83, br s
18	0.94, d (6.8)	0.94, d (6.6)	0.96, d (6.8)	0.94, d (6.8)	0.92, d (6.7)	0.93, d (6.9)	0.99, d (6.9)	0.97, d (6.9)	0.94, d (6.9)
19	0.98, d (6.8)	0.98, d (7.0)	1.01, d (6.9)	0.98, d (6.9)	0.97, d (6.6)	0.91, d (6.9)	1.04, d (6.6)	0.91, d (7.0)	0.88, d (6.9)
20	1.02, d (6.9)	1.02, d (6.9)	0.98, d (6.6)	0.96, d (6.6)	1.02, d (6.7)	1.01, d (6.9)	1.03, d (6.5)	1.03, d (7.2)	0.83, d (6.6)

[a] NMR data (500 MHz) in CD_2Cl_2.
[b] Full assignments were carried out by DEPT, gHMQC, and gHMBC experiments.

derivatization reagent, as described for **1**.[12,13] Selected differences in the chemical shift ($\Delta\delta^{RS}$) data for the (*R*)- and (*S*)-MPA esters at C-3 (**2a** and **2b**, respectively) are summarized in Table 3. Thus, the structure of **2** was established as (1*R*,3*R*,4*R*,8*R*,12*R*)-6,11-diketocembra-15(17)-en-3-ol [(8*R*)-plexaurolone]. This compound is a C-8 epimer of compound **1** and this is the first time that **2** has been reported in the chemical literature.

Compound **3** was isolated as optically active colorless crystals with a molecular formula assigned as $C_{20}H_{36}O_3$ on the basis of its HRESIMS pseudomolecular ion at m/z 347.2568 $[M+Na]^+$ (Δ 1.7 ppm) and ^{13}C NMR spectra, which indicated 3° of unsaturation. The IR spectrum revealed the presence of carbonyl (1689 cm^{-1}), hydroxyl (3433 cm^{-1}), and olefin (887 cm^{-1}) groups. The NMR data (Tables 1 and 2) for compound **3** (in CD_2Cl_2) showed spectroscopic

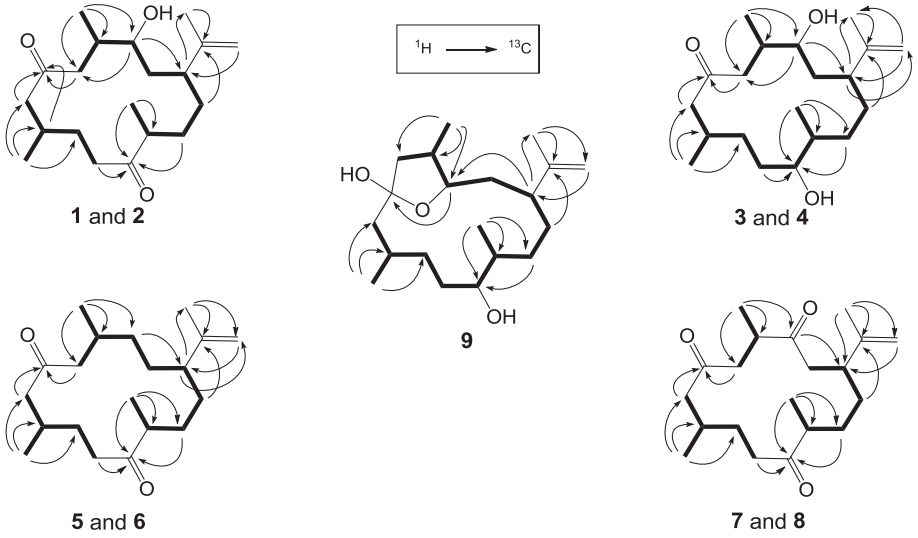

Fig. 1. ^{1}H–^{1}H COSY correlations (bold lines) and key gHMBC correlations (arrows) for compounds **1**–**9**.

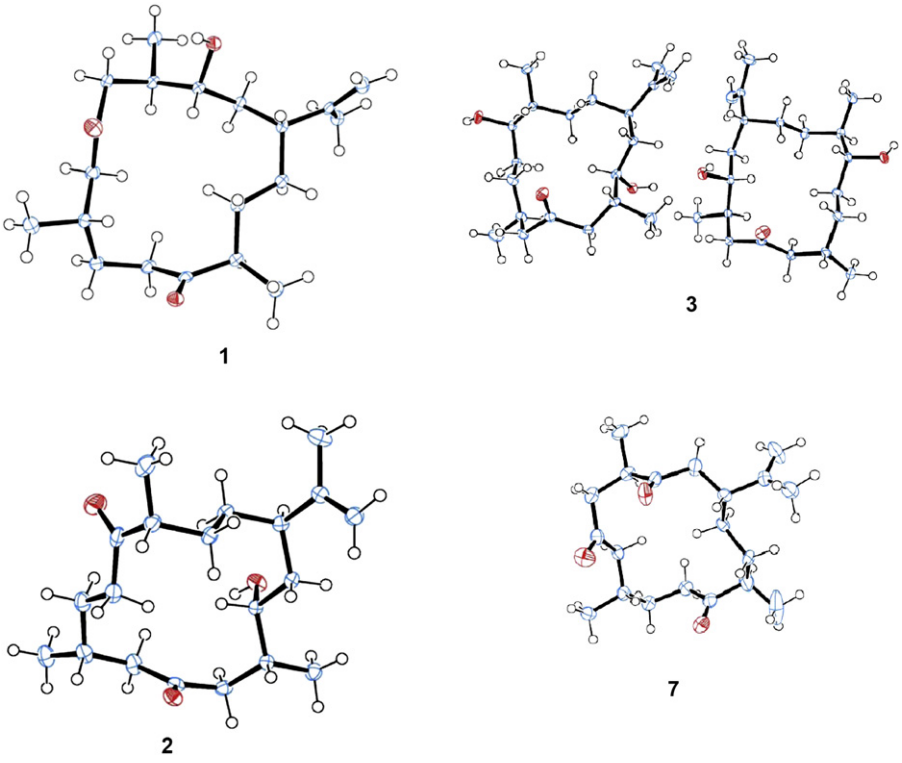

Fig. 2. ORTEP perspective drawings of compounds **1**–**3** and **7**.

Table 3
Selected ^{1}H NMR spectroscopic data (400 MHz, $CDCl_3$) for the MPA esters at C-3 for **1a**,**b**, **2a**,**b** and at C-11 for **4a**,**b**, **9a**,**b** and the $\Delta\delta^{RS}=\delta R-\delta S$ values obtained

No.	**1a**	**1b**	$\Delta\delta^{RS}$	**2a**	**2b**	$\Delta\delta^{RS}$	**4a**	**4b**	$\Delta\delta^{RS}$	**9a**	**9b**	$\Delta\delta^{RS}$
H-16	1.65, s	1.51, s	+0.140	1.63, s	1.60, s	+0.0.30	1.67, s	1.71, s	−0.040	1.67, s	1.71, s	−0.040
H-17a	4.68, br s	4.40, br s	+0.280	4.72, br s	4.32, br s	+0.400	4.64, br s	4.69, br s	−0.050	4.65, br s	4.68, br s	−0.030
H-17b	4.73, br s	4.58, br s	+0.160	4.76, br s	4.57, br s	+0.190	4.67, s	4.70, s	−0.030	4.67, s	4.70, s	−0.030
H-18	0.69, d, *J*=6.8 Hz	0.90, *J*=7.0 Hz	−0.210	0.97, d, *J*=6.8 Hz	1.27, *J*=7.0 Hz	−0.300	0.94, d, *J*=7.0 Hz	0.93, d, *J*=6.8 Hz	+0.010	0.94, d, *J*=7.3 Hz	0.93, d, *J*=6.9 Hz	+0.010
H-19	0.98, d, *J*=7.0 Hz	0.98, d, *J*=7.0 Hz	0.000	1.02, d, *J*=6.8 Hz	0.96, d, *J*=6.9 Hz	0.060	0.92, d, *J*=7.0 Hz	0.85, d, *J*=6.5 Hz	+0.070	0.92, d, *J*=7.2 Hz	0.85, d, *J*=6.6 Hz	+0.070
H-20	1.02, d, *J*=6.9 Hz	1.02, d, *J*=6.9 Hz	0.000	1.12, d, *J*=6.9 Hz	0.98, d, *J*=6.6 Hz	0.140	0.52, d, *J*=6.6 Hz	0.66, d, *J*=6.7 Hz	−0.140	0.52, d, *J*=6.7 Hz	0.65, d, *J*=6.7 Hz	−0.130
H-3	4.76, s	4.76, s	0.000	4.77, s	4.77, s	0.000	2.76, dd, *J*=16.0, 10.8 Hz	2.71, dd, *J*=15.9, 10.8 Hz	+0.050	2.76, dd, *J*>=16.0, 10.7 Hz	2.70, dd, *J*=16.0, 10.7 Hz	+0.060
H-4	2.12, m	2.40, m	−0.280	2.01, m	2.31, m	−0.300	—	—	—	2.27, m	2.27, m	0.000
H-5	2.58, m	2.65, m	−0.070	2.43, dd, *J*=15.5, 7.1 Hz	2.62, dd, *J*=14.4, 11.9 Hz	−0.190	2.42, m, *J*=14.6, 3.1 Hz	2.31, dd, *J*=14.7, 2.9 Hz	+0.050	2.04, m	2.04, m	0.000

features for a cembrane-type diterpene.[10,11] The spectra showed three methyl groups as aliphatic substituents (δ_H 1.01, d, J=6.9 Hz, δ_C 20.9; δ_H 0.98, d, J=6.6 Hz, δ_C 16.1; δ_H 0.96, d, J=6.8 Hz, δ_C 13.4) and one isopropenyl group (δ_H 1.75, s, δ_C 21.1, CH_3; δ_H 4.75, br s, 4.69, br s, δ_C 109.0, CH_2; δ_C 150.2, qC). Other signals associated with two hydroxy methine groups (δ_H 3.45, ddd, J=9.0, 6.4, 2.7 Hz, δ_C 70.1; δ_H 3.32, d, J=10.9 Hz, δ_C 75.0, qC) and one ketone group (δ_C 211.3, qC) were also observed. In the ^{1}H–^{1}H COSY spectrum it was possible to identify only one spin system, from H_2-5 passing through H-1 to H_2-7 (Fig. 1), which was assembled with the carbonyl at C-6 with the aid of a gHMBC experiment (H_2-5 and H_2-7 with C-6). Detailed analysis of ^{1}H–^{1}H COSY, gHMQC, and gHMBC data allowed the assignment of all NMR signals and established the planar structure of this compound (Tables 1 and 2, Fig. 1). The relative configuration of this cembrane was established as 1*R**,3*R**,4*R**,8*S**,11*R**,12*R** by single-crystal X-ray diffraction (Fig. 2).

On the other hand, when NMR spectra of compound **3** were recorded in $CDCl_3$, we observed the conversion of this compound to the cyclic hemiketal **9** (δ_C 109.7 for C-6 and δ_H 3.95, ddd, J=12.6, 7.0, and 2.4 Hz, δ_C 79.0 for C-3), probably due to the intramolecular nucleophilic addition of the hydroxyl at C-3 to the carbonyl ketone group at C-6 (Fig. 3). Further detailed analyses of ^{1}H–^{1}H COSY, gHMQC, and gHMBC data allowed us to assign the complete planar structure of compound **9** (Tables 1 and 2, Fig. 1). When compound **3** was dissolved in $CDCl_3$ and its ^{1}H NMR spectrum was quickly recorded, a mixture of compounds **3** and **9** was observed.

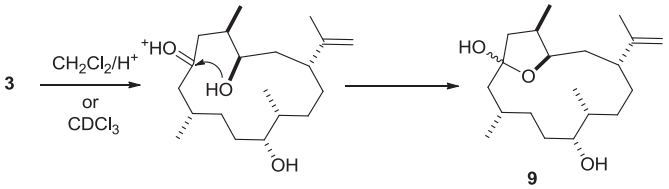

Fig. 3. Chemical interconversion of compound **3** into **9**.

In order to establish the absolute configuration of compound **3**, it was fully converted into **9** in situ by dissolving it in acidified CH_2Cl_2. Esterification of the hydroxyl group at C-11 of compound **9** with (*R*)- and (*S*)-MPA[12,13] gave the resulting pair of diastereoisomers (**9a** and **9b**, respectively), which were analyzed for differential ^{1}H NMR resonances. Selected chemical shift differences ($\Delta\delta^{RS}$) for **9a** and **9b** are summarized in Table 3. These data clearly establish the 11*R* configuration of **9**. Hence, the absolute configuration of the C-11 chiral center of natural compound **3** was determined to be *R* and this led us to establish its absolute stereochemistry as (1*R*,3*R*,4*R*,8*S*,11*R*,12*R*)-6-ketocembra-15(17)-en-3,11-diol [(8*S*)-dihydroplexaurolone]. Although the chemical shifts and the NMR assignments of compound **3** are consistent with those published for dihydroplexaurolone by Chan et al.,[9] their reported structures in the Chart 1 and in the ORTEP diagram are contradictory in terms of the relative stereochemistry at C-8 and C-11.

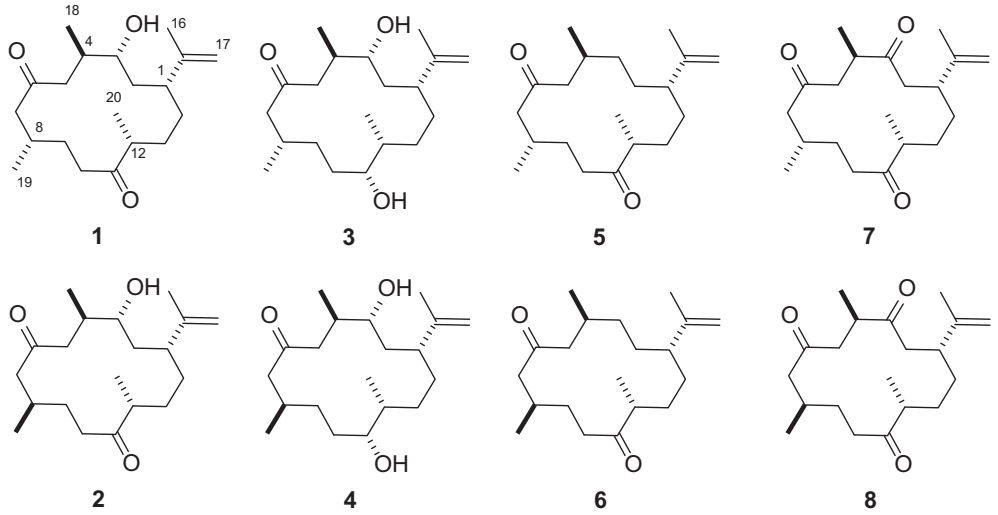

Chart 1.

Compound **4** has the molecular formula $C_{20}H_{36}O_3$ assigned on the basis of the HRESIMS pseudomolecular ion at *m*/*z* 347.2563 $[M+Na]^+$ (Δ 0.3 ppm) and the ^{13}C NMR data imply 3° of unsaturation. The IR spectrum revealed the presence of carbonyl (1689 cm^{-1}) and hydroxyl (3433 cm^{-1}) groups. The NMR data for compound **4** also showed spectroscopic features for a cembrane-type diterpene, i.e., 20 carbon signals, including three methyl groups (δ_H 0.98, d, *J*=6.9 Hz, δ_C 21.1; δ_H 0.96, d, *J*=6.6 Hz, δ_C 16.2; δ_H 0.94, d, *J*=6.8 Hz, δ_C 13.6) and one isopropenyl group (δ_H 1.70, s, δ_C 21.3, CH_3; δ_H 4.70, br s, 4.64, br s, δ_C 109.3, CH_2; δ_C 149.9, qC). In addition, signals assigned to one ketone group (δ_C 211.8, qC) and two hydroxy methine groups (δ_H 3.31, ddd, *J*=9.0, 6.4, 2.7 Hz, δ_C 75.1, CH; δ_H 3.43, d, *J*=10.9 Hz, δ_C 70.1, CH) were observed. In the ^{1}H–^{1}H COSY experiment, the long-range coupling between H_3-16 and H_2-17 corroborates the presence of an isopropenyl group. The position of the isopropenyl group was established by correlations of H_2-17 with C-1 and C-16, as well as H-1 with C-16 and C-17 in the gHMBC experiment, fixing the position of the isoprenyl group at C-1. It was possible to identify a single spin system, from H_2-5 passing through H-1 to H_2-7, which was assembled with the carbonyl at C-6 with the aid of a gHMBC experiment (H_2-5 and H_2-7 with C-6) (Fig. 1). The positions of other substituents were fixed by detailed analysis of ^{1}H–^{1}H COSY, gHMQC, and gHMBC data, which allowed assignment of the complete planar structure of this compound (Tables 1 and 2, Fig. 1) and showed it to be a stereoisomer of **3**. The relative configuration of cembranoid **4** was established as 1*R**,3*R**,4*R**,8*R**,11*R**,12*R** from NOESY analysis, particularly by the cross-peaks between H-11 and H-8, and H-3 with H-1/H_3-18. The absolute configuration of **4** was assigned using the modified Mosher method. Treatment of this compound with MPA as a derivatization reagent[12,13] afforded the C-11 (*R*)- and (*S*)-MPA esters of **4**. Selected data for chemical shift differences ($\Delta\delta$) are summarized in Table 3 and led us to establish the structure as (1*R*,3*R*,4*R*,8*R*,11*R*,12*R*)-6-ketocembra-15(17)-en-3,11-diol [(8*R*)-dihydroplexaurolone] for compound **4**. This compound is a C-8 epimer of compound **3** and this is the first time that **4** has been reported in the chemical literature. Interestingly, a solution of compound **4** in $CDCl_3$ did not afford the corresponding cyclic hemiketal, as occurred with **3**, indicating the importance of the stereochemistry at C-8 in the proposed intramolecular nucleophilic addition reaction.

Compounds **5** and **6** have the same molecular formula, i.e., $C_{20}H_{34}O_2$, as determined by the HRESIMS pseudomolecular ion at *m*/*z* 329.2456 $[M+Na]^+$ (Δ 0.3 ppm) for **5** and *m*/*z* 329.2454 $[M+Na]^+$ (Δ 0.9 ppm) for **6**, implying 4° of unsaturation in both cases. The IR spectra of these compounds revealed the presence of carbonyl (1705 cm^{-1}) and olefinic (1651 cm^{-1}) groups but no hydroxyl functionality. The NMR data for compound **5** showed spectroscopic features for a cembrane-type diterpene,[10,11] i.e., 20 carbon signals, including the presence of three methyl groups (δ_H 1.02, d, *J*=6.7 Hz, δ_C 16.6; δ_H 0.97, d, *J*=6.6 Hz, δ_C 20.3; δ_H 0.92, d, *J*=6.7 Hz, δ_C 21.0), an isopropenyl group (δ_H 4.70, br s, 4.62, br s, δ_C 110.0, CH_2; δ_H 1.63, s, δ_C 20.4, CH_3; δ_C 147.8, qC) and two ketone groups (δ_C 214.7, qC and δ_C 210.6, qC). Analysis of the ^{1}H–^{1}H COSY spectrum of **5** led us to establish two sets of spin systems, the longest from H_2-5 passing through H-1 to H_3-20 and the other from H_2-7 to H_2-10, which were connected with the ketone carbonyl groups C-6 and C-11 by a gHMBC experiment. Thus, key HMBC correlations between H_3-20, H_2-13 and H_2-10 with C-11 and H_2-7 and H_2-5 with C-6 led us fix the positions of the two carbonyl groups and allowed us to assign the complete planar structure for **5** and perform the assignment of all NMR signals (Tables 1 and 2, Fig. 1). Compound **6** exhibited similar NMR signals and spectroscopic correlations to compound **5** (Tables 1 and 2), with the exception of the signals assigned to CH_2-5 (δ_H 2.53, m, 2.32, m, δ_C 37.4, in **5**; δ_H 2.49, m, 2.18, m, δ_C 35.9, in **6**) and CH_2-10 (δ_H 2.13, m, 2.06, m, δ_C 47.8, in **5**; δ_H 2.35, m, 2.30, m, δ_C 50.5, in **6**), indicating that compound **6** is a stereoisomer of **5**. The relative configurations of **5** and **6** were established from NOESY experiments, which showed that **5** is (1*S**,4*S**,8*S**,12*R**)-dehydroxyplexaurolone and **6** is (1*S**,4*S**,8*R**,12*R**)-dehydroxyplexaurolone.

The absolute configuration of compound **5** was established by its chemical interconversion from **1**. Thus, derivatization of the C-2 hydroxyl group of **1** with mesyl chloride followed by reductive-elimination with $LiAlH_4$ in CH_2Cl_2 (Fig. 4) gave a compound that had identical spectroscopic data and chiroptical properties to those of natural **5**. Therefore, we assigned the structure of **5** as (1*S*,4*S*,8*S*,12*R*)-6,11-diketocembra-15(17)-ene [(8*S*)-dehydroxyplexaurolone].

The main differences between the data for these compounds are the signals assigned to CH_2-7 (δ_H 2.08, m; 2.01, m, δ_C 49.5, in **7**; δ_H 2.53, m, 2.27, m, δ_C 50.9, in **8**), CH_2-10 (δ_H 2.94, m, 2.47, m, δ_C 36.7, in **7**; δ_H 2.41, m, 2.32, m, δ_C 38.3, in **8**) and CH_3-19 (δ_H 1.04, d, J=6.6 Hz, δ_C 21.5, in **7**; δ_H 0.91, d, J=7.0 Hz, δ_C 22.0, in **8**), indicating that compound **8** must be a stereoisomer of **7**. NOESY experiments on compounds **7** and **8** along with the X-ray diffraction analysis of a crystal of **7** allowed us to determine the relative configuration of **7** as (1*R**,4*R**,8*S**,12*R**)-dehydroplexaurolone and of **8** as (1*R**,4*R**,8*R**,12*R**)-dehydroplexaurolone, which is an epimer of compound **7** at C-8.

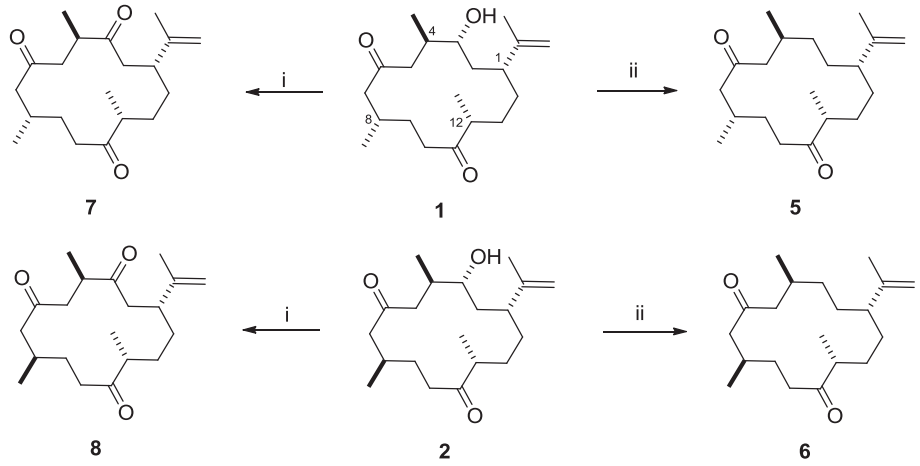

Fig. 4. Chemical interconversions of compounds **1** and **2** to **5**/**7** and **6**/**8**, respectively.

Following the same procedure as described for **5**, the chemical interconversion of **2** to a derivative with identical spectroscopic data and chiroptical properties to those of compound **6**, allowed us to establish its absolute stereochemistry as (1*S*,4*S*,8*R*,12*R*)-6,11-diketocembra-15(17)-ene [(8*R*)-dehydroxyplexaurolone]. The NMR data for compound **5** are coincident with those of a cembranoid isolated from *Eunicea mammosa* by Rodriguez et al.,[14] but a stereochemical specification was not established and the NMR data assignment was incomplete for the tentative structure reported. On the other hand, compound **6** is reported here in the chemical literature for the first time.

Compounds **7** and **8** were isolated as white needles and a colorless powder, respectively, and these compounds have the same molecular formula of $C_{20}H_{32}O_3$ based on the HRESIMS pseudomolecular ion at *m*/*z* 343.2246 $[M+Na]^+$ (Δ 0.3 ppm) for **7** and *m*/*z* 343.2248 $[M+Na]^+$ (Δ 0.3 ppm) for **8**, requiring 5° of unsaturation. The IR spectra revealed the presence of carbonyl (1705 cm^{-1}) and olefinic (1643 cm^{-1}) groups along with the absence of a hydroxyl functionality. The NMR data for compound **7** showed signals (Tables 1 and 2) for a cembrane-type diterpene,[10,11] i.e., three methyl groups, an isopropenyl group and three ketone groups (δ_C 215.6, qC; 214.4, qC; 210.4, qC). Analysis of the $^1H-^1H$ COSY spectra led us to establish three sets of spin systems: the first one comprising H_2-5/H-4/H_3-18, another one from H_2-7 to H_2-10 including H_3-19 and the last one from H-12 to H_2-14/H-1 to H_2-2 including H_3-20, and these were connected with the carbonyl groups at C-6, C-11, and C-3. Analysis of the key correlations in a gHMBC experiment, H_3-18 with C-3, H_2-7 and H_2-5 with C-6 and finally H_3-20, H_2-13 and H_2-10 with C-11, led us to fix these positions and establish the planar structure of **7** (Fig. 1). In a similar way, analysis of the 2D NMR data for compound **8** showed that this compound is a stereoisomer of compound **7**. The 2D NMR data for both compounds allowed us to relate all the protons to their corresponding carbons and perform the complete assignment of these compounds (Tables 1 and 2).

The absolute configurations of compounds **7** and **8** were established since their spectroscopic data and chiroptical properties are identical to those of the PCC oxidation products obtained from 8*S*-plexaurolone (**1**) and 8*R*-plexaurolone (**2**), respectively (Fig. 4). Thus, we assigned the structure of **7** as (1*R*,4*R*,8*S*,12*R*)-3,6,11-triketocembra-15(17)-ene [(8*S*)-dehydroplexaurolone] and that of **8** as (1*R*,4*R*,8*R*,12*R*)-3,6,11-triketocembra-15(17)-ene [(8*R*)-dehydroplexaurolone].

The NMR data for compound **7** are coincident with those of dehydroplexaurolone published by Chan et al.,[9] but the stereochemistry at C-8 and the ^{13}C NMR data assignments were revised. On the other hand, the NMR data for compound **8** are coincident with those of a second dehydroplexaurolone published by the same authors,[9] but stereochemical specifications were established at C-4 and C-12. We resolved the absolute configuration at these chiral centers and the configuration at C-8 and ^{13}C NMR data assignments were revised.

Antifouling activities of the natural compounds (**1**–**8**) were evaluated using Quorum Sensing Inhibition (QSI) and biofilm inhibition assays. For QSI activity, *Chromobacterium violaceum* ATCC 31532 biosensor strain was used. The results reveal that compounds **3** (7.5 μg/disk) and **6** (7.5 μg/disk) had a significant inhibitory effect on QS-regulated violacein pigment production in *C. violaceum* without interfering with its growth (Table 4). Compound **7** (30.0 μg/disk) showed moderate activity. As growth was not inhibited by these compounds, we assumed that the negative effect on violacein production is caused by disruption of the QS signaling system. Avoiding a bactericidal effect, this result represents a highly encouraging approach because there is no selective pressure for the development of resistance in bacteria. Compounds **3**, **6**, and **7** disrupted QS systems at lower concentrations than cuprous oxide. This compound is commonly used as commercial antifoulant.

Table 4
QSI activity of compounds **1**–**8**

Specie	*Chromobacterium violaceum*
Compounds	Inhibition of QS (quantity in μg/disk)[a]
1	—
2	—
3	7.5
4	—
5	—
6	7.5
7	30.0
8	—
Solvent	—
Cu_2O	40.0

Activity was measured by the inhibition of violacein pigment.
—No zone of inhibition even at 30 μg/disk.
[a] Minimum quantity in μg per disk of compound required to inhibit violacein pigment.

Pseudomonas aeruginosa, *Vibrio harveyi*, and *Staphylococcus aureus* were used for biofilm inhibition assays and compounds were evaluated at (a) 2.5, (b) 10, and (c) 100 ppm. The results show that all compounds (**1**–**8**) inhibited completely the biofilm maturation of *P. aeruginosa* at 100 ppm but they did not present significant activity at the lowest concentrations (Fig. 5A). Epimers 8*S* showed selective activity against *V. harveyi*. In particular, compounds **3** and **5** at 10 ppm inhibited biofilm maturation by more than 75%, compound **7** at 100 ppm gave an inhibition of 40% and stereoisomer **8** at 100 ppm exhibited biofilm inhibition of about 95% (Fig. 5B). Finally, stereoisomers 8*R* showed selective biofilm inhibition activity against a Gram positive bacterium (*S. aureus*); in particular, compounds **4**, **6**, and **8** at 10 ppm exhibited inhibition of biofilm maturation of about 70% and epimer **5** also showed 70% biofilm inhibition against *S. aureus* at 10 ppm (Fig. 5C). On the other hand, some compounds promoted biofilm maturation, as shown in Fig. 5. It is noteworthy that the inhibition of biofilm in all cases was achieved without interference in its growth, even at 100 ppm (see Supplementary data, Fig. S20). The fact that compounds **3** and **6** presented QSI and biofilm inhibition activities suggests that these compounds may interfere in bacterial communication, thus avoiding biofilm maturation and the successive development of microbial communities. This action would consequently affect the association of other species to the surface, which could probably avoid later steps in the fouling process.[15,16]

In summary, we have isolated eight antifouling compounds (four pairs of epimers) with a cembrane-type skeleton and, among these, compounds **2**, **4**, and **6** are reported for the first time in the chemical literature. Additionally, we have reported or revised the relative and absolute stereochemistries and have obtained complete NMR assignments for compounds **1**, **3**, **5**, **7**, and **8**. The properties of all compounds against microfouling were measured and it was found that compounds **3** and **6** are the most active. It is noteworthy that these compounds exhibit biofilm inhibition values in the order of 2.5 ppm.[1]

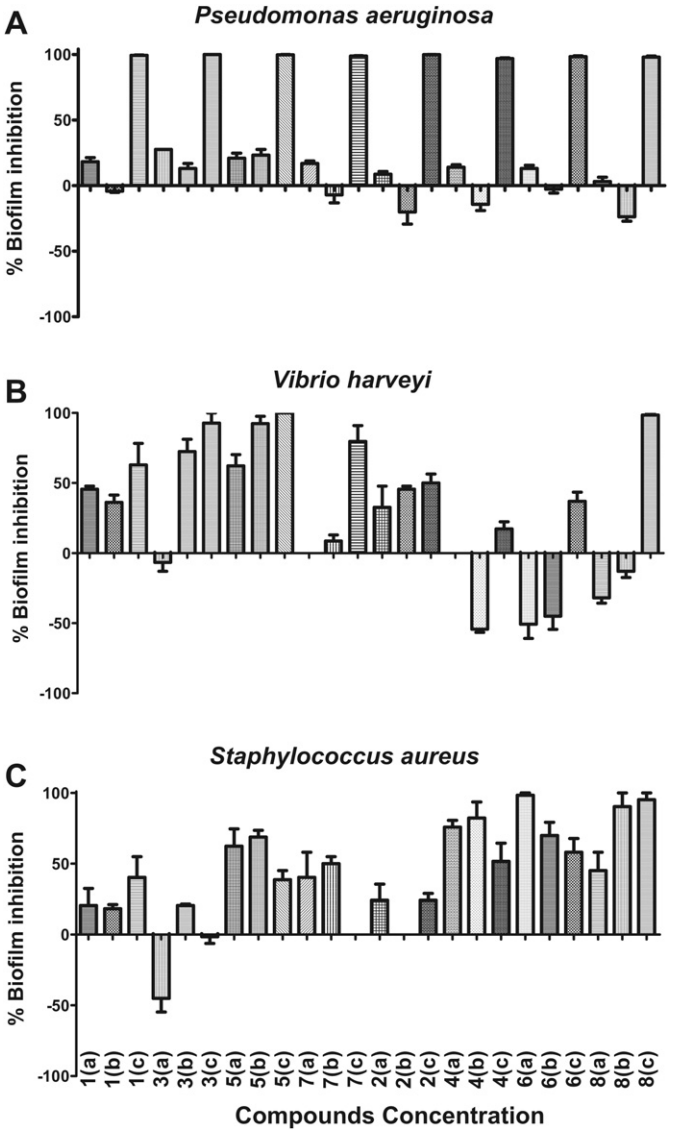

Fig. 5. Inhibition of biofilm maturation by compounds **1**–**8** against (A) *P. aeruginosa*, (B) *V. harveyi*, and (C) *S. aureus*. Compounds were evaluated at (a) 2.5 ppm, (b) 10 ppm and (c) 100 ppm.

3. Experimental section

3.1. General experimental procedures

Optical rotations were measured on a Polartronic ADP440+, Bellinghan+stanley polarimeter. IR spectra were recorded on a Perkin–Elmer FT-IR Paragon 500, series 1000 spectrophotometer. ^{1}H and ^{13}C NMR (one- and two-dimensional) spectra were recorded on a Bruker Avance 400 (400 MHz for ^{1}H and 100 MHz for ^{13}C) spectrometer and on a Bruker Avance 500 spectrometer at 500 and 125 MHz, respectively, using $CDCl_3$ or CD_2Cl_2 as solvents unless otherwise stated and with TMS as internal standard. The chemical shifts are given in δ and coupling constants in hertz. HRESIMS was performed on a VG Autospec-Bruker spectrometer with an ESI probe. Preparative HPLC was conducted on a Merck-Hitachi instrument with a UV–vis L-4250 detector (detected at 210 nm) using a LichroCART RP-18 (250×10 mm i.d., 10 μm) column, with MeOH/H_2O (80:20 v/v) as eluent at a flow rate of 2.5 mL/min. The absorbance was measured on a microelisa scanner sensident scan-Merck to establish the biofilm inhibition.

3.2. Animal material

The octocoral *P. flagellosa* was collected at Santa Marta Bay, Colombian Caribbean by SCUBA diving at a depth of 8 m. The fresh coral colonies were frozen immediately after collection and remained so until the extraction. Animals were identified by Prof. Dr. M. Puyana of Universidad Jorge Tadeo Lozano, and voucher specimens coded as ICN-MHN-PO 0257 were deposited at the invertebrate collection of the Instituto de Ciencias Naturales de la Universidad Nacional de Colombia.

3.3. Isolation and identification of compounds

The octocoral (360 g) was cut into small pieces and repeatedly extracted with a MeOH/CH_2Cl_2 (1:1 v/v) mixture. The resulting extract was filtered and concentrated by rotary evaporation to give a dark green oily extract (65 g), which was partitioned between CH_2Cl_2/H_2O (1:1 v/v). A portion of the organic fraction obtained (30 g) was subjected to silica gel vacuum column chromatography, eluting with 500 mL of solvents of increasing polarity [benzene (100%), benzene/EtOAc (90:10, 70:30, 50:50, 30:70 v/v), EtOAc (100%), EtOAc/MeOH (80:20, 50:50 v/v)] to obtain thirteen fractions (F1–F13). Antifouling activity assays of these fractions showed that F6, F8, F9, and F10 were the most active.

Fraction F6 (4 g) (eluted with benzene/EtOAc 70:30 v/v) was further subjected to silica gel flash column chromatography, eluting with benzene/EtOAc 95:5 v/v. Seventy two fractions (each ~15 mL) were collected and combined in seven subfractions (F6.1–F6.7). Subfraction F6.2 was repeatedly subjected to silica gel flash column chromatography with benzene/EtOAc 95:5 v/v to obtain pure compound **6** (460 mg). In addition, F6.3, F6.4, and F6.6 were submitted separately for final purification to reverse-phase HPLC, using MeOH/H_2O (80:20 v/v) as eluent, to afford pure compounds **5** (50 mg), **7** (530 mg), and **8** (24 mg), respectively. Fraction F8 (2 g) (eluted with benzene/EtOAc 50:50 v/v) was subjected to column chromatography under pressure on silica gel, using hexane/EtOAc 80:20 v/v as the mobile phase. One hundred and eighteen fractions (each ~15 mL) were collected and combined in six subfractions (F8.1–F8.6). Of these subfractions, F8.4 was repeatedly subjected to crystallization from EtOAc to afford pure compound **1** (991 mg). Furthermore, F8.3 was finally purified by reversed-phase HPLC, using MeOH/H_2O (70:30 v/v) as eluent, to yield pure compound **2** (10 mg), and F9 (eluted with benzene/EtOAc 30:70 v/v) and F10 (eluted with EtOAc 100%) were submitted to crystallization from EtOAc to afford pure compounds **4** (50 mg) and **3** (800 mg), respectively.

*3.3.1. (8S)-Plexaurolone (**1**).* White crystals; $[\alpha]_D^{25}$ −6.6 (*c* 0.23, $CHCl_3$); IR (KBr), ν_{max} 3417, 1697, 1643, 879 cm^{-1}; ^1H and ^{13}C NMR data, see Tables 1 and 2, respectively; ESIMS *m/z* 345 $[M+Na]^+$; HRESIMS *m/z* 345.2385 $[M+Na]^+$ (calcd for $C_{20}H_{34}O_3Na$, 345.2406).

*3.3.2. (8R)-Plexaurolone (**2**).* White crystals; $[\alpha]_D^{25}$ +18.0 (*c* 0.22, $CHCl_3$); IR (KBr), ν_{max} 3417, 1697, 1643, 879 cm^{-1}; ^1H and ^{13}C NMR data, see Tables 1 and 2, respectively; ESIMS *m/z* 345 $[M+Na]^+$; HRESIMS *m/z* 345.2386 $[M+Na]^+$ (calcd for $C_{20}H_{34}O_3Na$, 345.2406).

*3.3.3. (8S)-Dihydroplexaurolone (**3**).* White crystals; $[\alpha]_D^{25}$ +49.0 (*c* 0.25, CH_2Cl_2); IR (KBr), ν_{max} 3433, 1689, 1643, 887 cm^{-1}; ^1H and ^{13}C NMR data, see Tables 1 and 2, respectively; ESIMS *m/z* 347 $[M+Na]^+$; HRESIMS *m/z* 347.2568 $[M+Na]^+$ (calcd for $C_{20}H_{36}O_3Na$, 347.2562).

*3.3.4. (8R)-Dihydroplexaurolone (**4**).* White crystals; $[\alpha]_D^{25}$ +40.5 (*c* 0.29, $CHCl_3$); IR (KBr), ν_{max} 3433, 1689, 1643, 887 cm^{-1}; ^1H and ^{13}C NMR data, see Tables 1 and 2, respectively; ESIMS *m/z* 347 $[M+Na]^+$; HRESIMS *m/z* 347.2563 $[M+Na]^+$ (calcd for $C_{20}H_{36}O_3Na$, 347.2562).

*3.3.5. (8S)-Dehydroxyplexaurolone (**5**).* Colorless powder; $[\alpha]_D^{25}$ −4.8 (*c* 0.23, $CHCl_3$); IR (KBr), ν_{max} 1705, 1651, 887 cm^{-1}; ^1H and ^{13}C NMR data, see Tables 1 and 2, respectively; ESIMS *m/z* 329 $[M+Na]^+$; HRESIMS *m/z* 329.2456 $[M+Na]^+$ (calcd for $C_{20}H_{34}O_2Na$, 329.2457).

*3.3.6. (8R)-Dehydroxyplexaurolone (**6**).* Colorless powder; $[\alpha]_D^{25}$ +3.0 (*c* 0.22, $CHCl_3$); IR (KBr), ν_{max} 1705, 1651, 887 cm^{-1}; ^1H and ^{13}C NMR data, see Tables 1 and 2, respectively; ESIMS *m/z* 329 $[M+Na]^+$; HRESIMS *m/z* 329.2454 $[M+Na]^+$ (calcd for $C_{20}H_{34}O_2Na$, 329.2457).

*3.3.7. (8S)-Dehydroplexaurolone (**7**).* Yellow needles; $[\alpha]_D^{25}$ +6.8 (*c* 0.40, $CHCl_3$); IR (KBr), ν_{max} 1705, 1643, 887 cm^{-1}; ^1H and ^{13}C NMR data, see Tables 1 and 2, respectively; ESIMS *m/z* 343 $[M+Na]^+$; HRESIMS *m/z* 343.2246 $[M+Na]^+$ (calcd for $C_{20}H_{32}O_3Na$, 343.2249).

*3.3.8. (8R)-Dehydroplexaurolone (**8**).* Colorless powder; $[\alpha]_D^{25}$ −3.3 (*c* 0.21, $CHCl_3$); IR (KBr), ν_{max} 1705, 1643, 887 cm^{-1}; ^1H and ^{13}C NMR data, see Tables 1 and 2, respectively; ESIMS *m/z* 343 $[M+Na]^+$; HRESIMS *m/z* 343.2248 $[M+Na]^+$ (calcd for $C_{20}H_{32}O_3Na$, 343.2249).

*3.3.9. (1R,3R,4R,8S,11R,12R)-3,6-Oxa-cembra-15(17)-en-6,11-diol (**9**).* White crystals; $[\alpha]_D^{25}$ +49.0 (*c* 0.25, $CHCl_3$); IR (KBr), ν_{max} 3433, 1689, 1643, 887 cm^{-1}; ^1H and ^{13}C NMR data, see Tables 1 and 2, respectively; ESIMS *m/z* 347 $[M+Na]^+$; HRESIMS *m/z* 347.2568 $[M+Na]^+$ (calcd for $C_{20}H_{36}O_3Na$, 347.2562).

3.4. Crystallographic data and X-ray structure analysis of 1–3 and 7

Small colorless plates of **1**, **2**, and **3** were grown by the slow evaporation of a CH_3CN solution. Data were collected using an X8 APEX II BRUKER-NONIUS diffractometer equipped with a KYROFLEX low-temperature apparatus operating at 100 K. A suitable crystal was chosen and mounted on Mitegen MicroMount (radiation-hard polymer). Data were measured using omega scans of 0.5% per frame for 10 s, such that a total of 2382 frames were collected in a wide strategy and with a final resolution of 0.785%A. Data integration and reduction were performed using the Apex2 Service v2010, 1–2 (BRUKER AXS) software suite. Absorption corrections were applied using SADABS (2008) incorporated in the software suite. The structures were solved by the direct method using SHELX-XS Version 2008/1 and refined by the least squares method on F2 SHELXL Version 2008/4, incorporated in the Apex2 software suite.

*3.4.1. (8S)-Plexaurolone (**1**).* The full-matrix least-squares refinement (on F^2) of 213 variables converged to values of the conventional crystallographic residuals *R*1=0.0301 (*wR*2=0.0809) for data with $[I>2\sigma(I)]$ and *R*1=0.0348 (*wR*2=0.0829) for all data. The goodness-of-fit on F^2 was 1.367.

Crystal data: colorless block: 0.42×0.35×0.16 mm; orthorhombic; space group $P2_12_12_1$; unit cell dimensions *a*=8.2215, *b*=13.2649, *c*=17.1484 Å, *V*=1870.16 $Å^3$, *Z*=4, d_{calcd}=1.145 Mg m^{-3}.

*3.4.2. (8R)-Plexaurolone (**2**).* The full-matrix least-squares refinement (on F^2) of 213 variables converged to values of the conventional crystallographic residuals *R*1=0.0458 (*wR*2=0.1162) for data with $[I>2\sigma(I)]$ and *R*1=0.0397 (*wR*2=0.1095) for all data. The goodness-of-fit on F^2 was 0.975.

Crystal data: colorless block: 0.50×0.09×0.05 mm; monoclinic; space group $P2_1$; unit cell dimensions *a*=5.2009 *b*=18.5086, *c*=9.9092 Å, α=γ=90, β=103.4814, *V*=927.59 $Å^3$, *Z*=2, d_{calcd}=1.155 Mg m^{-3}.

*3.4.3. (8S)-Dihydroplexaurolone (**3**).* The full-matrix least-squares refinement (on F^2) of 427 variables converged to values of the conventional crystallographic residuals *R*1=0.0357 (*wR*2=0.0904) for data with $[I>2\sigma(I)]$ and *R*1=0.0331 (*wR*2=0.0882) for all data. The goodness-of-fit on F^2 was 1.017.

Crystal data: colorless block: 0.37×0.34×0.28 mm; monoclinic; space group $P2_1$; unit cell dimensions *a*=10.6225 *b*=10.8495, *c*=16.9084 Å, α=γ=90, β=99.916, *V*=1919.56 $Å^3$, *Z*=4, d_{calcd}=1.123 Mg m^{-3}.

*3.4.4. (8S)-Dehydroplexaurolone (**7**).* The full-matrix least-squares refinement (on F^2) of 231 variables converged to values of the conventional crystallographic residuals $R1$=0.0514 ($wR2$=0.1352) for data with [$I>2\sigma(I)$] and $R1$=0.0692 ($wR2$=0.1243) for all data. The goodness-of-fit on F^2 was 1.025.

Crystal data: yellow needle: 0.49×0.07×0.04 mm; monoclinic; space group $P2_12_12_1$; unit cell dimensions a=5.6582, b=17.7897, c=18.6316 Å, α=β=γ=90, V=1875.41 Å^3, Z=4, d_{calcd}=1.135 Mg m^{-3}.

3.5. Chemical transformations

*3.5.1. Conversion of 8R-plexaurolone (**2**) into 8R-dehydroplexaurolone (**8**).* Compound **2** (20.0 mg) was treated with PCC (24 mg) in dry CH_2Cl_2 (1 mL) for about 2 h with stirring at room temperature.[7] The reaction was quenched by the addition of water (3 mL). The organic layer was concentrated to dryness. The residue was purified by column chromatography [SiO_2, benzene/EtOAc (9:1)] to obtain a product identical to **8**. The purified product (15.8 mg), a colorless powder with an $[\alpha]_D^{25}$ −3.2 (*c* 0.15, $CHCl_3$), presented ^{1}H NMR data that matched those obtained for **8** (Table 2).

*3.5.2. Conversion of (8S)-plexaurolone (**1**) into (8S)-dehydroplexauralone (**7**).* Compound **1** (20.0 mg) was treated in the same way as described for **2**. The purified product (18.0 mg) was a colorless powder; $[\alpha]_D^{25}$ +10.0 (*c* 0.22, $CHCl_3$), the ^{1}H NMR data matched those exhibited by **7** (Table 2).

*3.5.3. Conversion of (8R)-plexaurolone (**2**) into (8R)-dehydroxyplexaurolone (**6**).* Mesylation of **2** (20.0 mg) was carried out using MsCl (13.0 mg) in dry pyridine (2 mL) with stirring at room temperature for 6 h.[3] Ice and H_2O were added to the reaction mixture and the product was extracted with CH_2Cl_2 (3×1 mL). The organic layer was separated and concentrated by rotary evaporation. The residue was treated with $LiAlH_4$ (3.0 mg) in dry THF (2 mL) at room temperature. After 10 h, the mixture was treated dropwise with a saturated Na_2SO_4 solution. The final mixture was filtered and purified by column chromatography [benzene/EtOAc (9:1 v/v)] to obtain a pure product identical to **6**. The purified product (3.2 mg) was a colorless powder; $[\alpha]_D^{25}$ +3.1 (*c* 0.23, $CHCl_3$), the ^{1}H NMR data matched those exhibited by **6** (Table 2).

*3.5.4. Conversion of (8S)-plexaurolone (1) into (8S)-dehydroxyplexaurolone (**5**).* Compound **1** (20.0 mg) was treated in the same way as described for compound **2**. The purified product (2.8 mg) was a colorless powder; $[\alpha]_D^{25}$ −4.4 (*c* 0.22, $CHCl_3$), the ^{1}H NMR data matched those exhibited by **5** (Table 2).

*3.5.5. Conversion of (8S)-dihydroplexaurolone (**3**) into **9**.* Compound **3** was dissolved in acidified CH_2Cl_2 (3 mL of CH_2Cl_2 with ten drops of acetic acid). The in situ transformation of **3** into compound **9** was followed by changes in R_f on TLC.

*3.5.6. Preparation of (R)- and (S)-MPA esters **1a**,**b** and **2a**,**b** from compounds **1** and **2**.* Ester derivatives **1a**,**b** and **2a**,**b** were prepared by treating separately compounds **1** and **2** (2.0 mg) with (*R*)- and (*S*)-MPA (1.2 mg), respectively, in dry methylene chloride (1 mL) in the presence of DCC (3.4 mg) and DMAP (catalytic amount) at room temperature for 24 h.[12,13] Each reaction mixture was filtered and the resulting ester was purified by reversed phase-HPLC (Lichro-CART RP-18). For selected ^{1}H NMR data for derivatives **1a**,**b** and **2a**,**b**, see Table 3.

*3.5.7. Preparation of (R)- and (S)-MPA esters **4a**,**b** and **9a**,**b** from compounds **4** and **9**.* *R*- and *S*-MPA ester derivatives **4a**,**b** and **9a**,**b** were prepared from **4** and **9**, respectively, in the same way as described for compounds **1** and **2**. For selected ^{1}H NMR data for derivatives **4a**,**b** and **9a**,**b**, see Table 3.

3.6. Evaluation of antifouling activities

3.6.1. Quorum sensing inhibition (QSI) assay. A standard disk-diffusion assay was used to evaluate QSI activity of compounds **1**–**8**, following the guidelines of the NCCLS,[17] using the biosensor strain *C. violaceum* (ATCC 31532) grown in trypticase soy agar as required. Whatman filter paper disks (5.2 mm diameter) were initially sterilized at 10×10^4 Pa pressure for 15 min. Disks were loaded with 30.0, 15.0, 7.5, 5.0, and 2.5 μg of each compound previously dissolved in MeOH and allowed to dry at room temperature during 1 h. The samples were placed on agar dishes plated with 100 μL of *C. violaceum* culture grown in trypticase soy broth (10^6 cf.u/mL, 0.5 Mac Farland). Agar plates were incubated 24 and 48 h at 26 °C and the activity was evaluated by measuring the diameter (*D*, in mm) of the inhibition zones around disks. QSI was detected by a colorless, opaque, but viable halo.[18]

3.6.2. Biofilm inhibition activity assay. Biofilm formations were performed in polystyrene microtitre dishes (96 wells), *V. harveyi*, *P. aeruginosa*, and *S. aureus* pre-inoculums were grown in LB, to an OD 600 nm of 0.2–0.3. Twenty microliters of each bacterium suspension was inoculated in each well and mixed with three different concentrations [(a) 2.5, (b) 10, and (c) 100 ppm] of pure compounds **1**–**8**. Finally, each well was completed with culture medium up to 200 μL. Microplates were incubated for 48 h at 37 °C. After discarding the medium by inversion, the wells were rinsed three times with distilled water (each 200 μL/well). Remaining adherent bacteria were stained for 5 min with 200 μL/well of violet crystal (1%), which was later discarded by inversion and wells were rinsed twice with distilled water (each 200 μL/well). In order to dissolve the colorant, a solution of ethanol/acetone (200 μL, 80:20 v/v) was added and after 10 min, the differential staining absorbance was quantified at 621 nm using a microelisa scanner sensident scan-Merck. For each experiment, correction for background staining was carried out by subtracting the absorbance of a blank (violet crystal bound to uninoculated wells). The absorbance value for bacterial culture staining without any compound was used as a baseline to calculate biofilm inhibition. Control of growth inhibition was monitored by measuring the absorbance of every well at 621 nm before and after incubation.

Acknowledgements

This work was financially supported by grants from Colciencias and DIB (Colombia), the Ministerio de Ciencia e Innovación (Spain), CTQ2008-04024/BQU and AGL2009-12266-C02-02 and Xunta de Galicia (Spain) (10PXIB253157PR). We thank Colciencias for a fellowship to support E.T. The authors would like to express their gratitude to Prof. Dr. Sven Zea for the collection of the animal samples and to Prof. Dr. M. Puyana for morphological identification of specimens used in this study. The Ministerio de Ambiente, Vivienda y Desarrollo Territorial granted permission (Permission No. 4 of 10/02/2010) to collect samples and perform research on marine organisms collected at Santa Marta Bay and at the Rosario Islands, Colombian Caribbean.

Supplementary data

^{1}H and ^{13}C NMR spectra of compounds **1**–**8**, and the effects of compounds **1**–**8** on the growth of *P. aeruginosa*, *V. harveyi*, and *S. aureus*. Supplementary data associated with this article can be found, in the online version, at doi:10.1016/j.tet.2011.09.094.

References and notes

1. Fusetani, N. *Acta Crystallogr.* **2011**, *28*, 400.
2. Mattmann, M. E.; Blackwell, H. E. *J. Org. Chem.* **2010**, *75*, 6737.
3. Tello, E.; Castellanos, L.; Arévalo-Ferro, C.; Duque, C. *J. Nat. Prod.* **2009**, *72*, 1595.
4. Cuadrado, C. T.; Castellanos, L.; Osorno, O.; Ramos, F. A.; Duque, C.; Puyana, M. *Quim. Nova* **2010**, *33*, 656.
5. Mayorga, H.; Urrego, N. F.; Castellanos, L.; Duque, C. *Tetrahedron Lett.* **2011**, *52*, 2515.
6. Weinheimer, A. J.; Matson, J. A. *Lloydia* **1975**, *38*, 378.
7. Reynolds, W. F.; McLean, S.; D'Armas, H. T.; Mootoo, B. S. *Magn. Reson. Chem.* **2001**, *39*, 94.
8. Ealick, S. E.; Van der Helm, D.; Gross, R. A.; Weinheimer, A. J.; Cieresako, L. S.; Middlebrook, R. E. *Acta Crystallogr.* **1980**, *B36*, 1901.
9. Chan, W. R.; Tinto, W. F.; Manchand, P. S.; Todaro, L. S.; Ciereszko, L. S. *Tetrahedron* **1989**, *45*, 103.
10. Mattern, M. L.; Scott, W. D.; McDaniel, C. A.; Weldon, P. J.; Graves, D. E. *J. Nat. Prod.* **1997**, *60*, 828.
11. Marville, K. I.; McLean, S.; Reynolds, W. F.; Tinto, W. F. *J. Nat. Prod.* **2003**, *66*, 1284.
12. Seco, J. M.; Quiñoa, E.; Riguera, R. *Chem. Rev.* **2004**, *104*, 17.
13. Seco, J. M.; Quiñoa, E.; Riguera, R. *Tetrahedron: Asymmetry* **2001**, *12*, 2915.
14. Rodriguez, A. D.; Li, Y.; Dhasmana, H. *J. Nat. Prod.* **1993**, *56*, 1101.
15. Dobretsov, S.; Teplitski, M.; Valerie, P. *Biofouling* **2009**, *25*, 413.
16. Briand, J. F. *Biofouling* **2009**, *25*, 297.
17. National Committee for Clinical Laboratory Standards. Performance standards for antimicrobial disk susceptibility test. Fourteenth Informational Supplement. NCCLS document M100-514. NCCLS, Wayne, PA, 2004.
18. Fotso, S.; Zabriskie, T. M.; Proteau, P. J.; Flatt, P. M.; Santosa, D. A.; Sulastri, M. T. *J. Nat. Prod.* **2009**, *72*, 690.